3.2. Gamma-ray response

The typical energy spectra of Ce 1%:GAGG excited by ^{137}Cs at 19 °C and measured using the APD are shown in Fig. 3. The light yield (LY) of the samples were calibrated from the ^{55}Fe direct irradiation peak to the APD. Such direct irradiation generates 5.9 keV/3.6 eV = 1630 electron-hole pairs. After correcting the QE, which is at 80% at 520 nm, the total LY becomes ~58,000 photon/MeV in $x = 2.7$ crystal. Energy resolution of the $x = 2.3$ was 4.2%@662 keV. Fig. 4 shows decay curves of the samples. Decay time was accelerated with increasing Ga concentration. Table 1 shows relationship between Ga concentrations, light yield, energy resolution and decay time. Light yield has maximum value at $x = 2.7$ Ga concentration and energy resolution became better with decreasing Ga concentration. Non-proportionality of the samples are shown in Fig. 5. The $x = 2.4$ sample showed the best non-proportionality among the obtained samples. This is good agreement with the result of the best energy resolution in $x = 2.4$ sample.

3.3. Single crystal X-ray structure analysis

The garnet structure has a cubic symmetry (Ia3d) with the general chemical formula $C_3A_2D_3O_{12}$. The ions D are surrounded by a dodecahedron of eight O^{2-} ions, the ions A are surrounded by an octahedron of O^{2-} ions, and the ions D are surrounded by an O^{2-} tetrahedron as shown in Fig. 6. By ionic size considerations the doping RE ions predominantly enter in the dodecahedral C-sites while the D-elements enter in octahedral and/or tetrahedral sites of the garnet lattice. In case of GAGG the C species are Gd^{3+} ions, while both A and D species are randomly occupied by Ga^{3+} and Al^{3+} ions [2,3,10]. Here, ionic radii of Al^{3+} (IV), Al^{3+} (VI), Ga^{3+} (IV) and Ga^{3+} (VI) are 0.39, 0.54, 0.47 and 0.62 respectively (see Fig. 7).

Single crystals were cut from the ingots and then carefully shaped into tiny spheres with diameters of 130–160 μm using Bond's method [6]. Diffraction intensity data were collected using

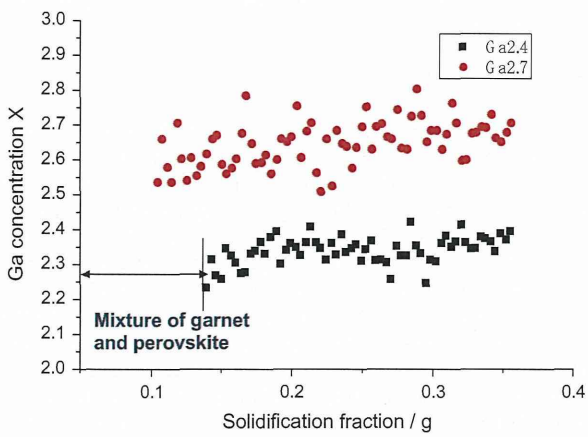

Fig. 3. Ga distributions of the grown $x = 2.4$ and 2.7 along the growth direction.

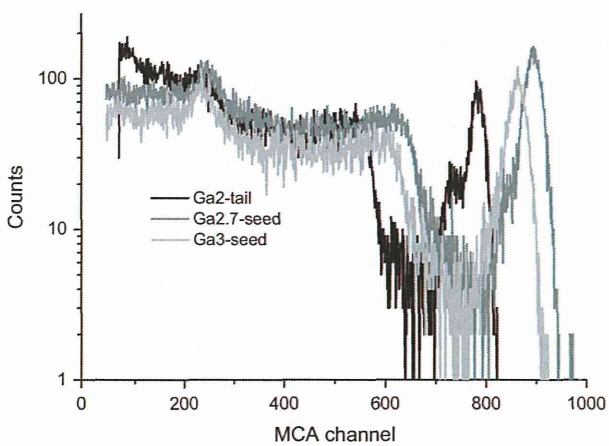

Fig. 4. Energy spectra of Ce 1%:GAGG samples excited by a 662 keV gamma-ray using the APD at 19 °C.

Table 1
Scintillation properties of the samples.

Ga concentrations	Emission wavelength /(nm)	Light yield (photon/MeV)	Energy resolution / (%@662 keV)	Decay time (ns)
3	520	55,000	5.2	97 ns(80%) 353 ns(20%)
2.7	516	58,000	4.8	172 ns(88%) 1932 ns(12%)
2.4	510	46,000	4.2	138 ns(71%) 649 ns(2%)

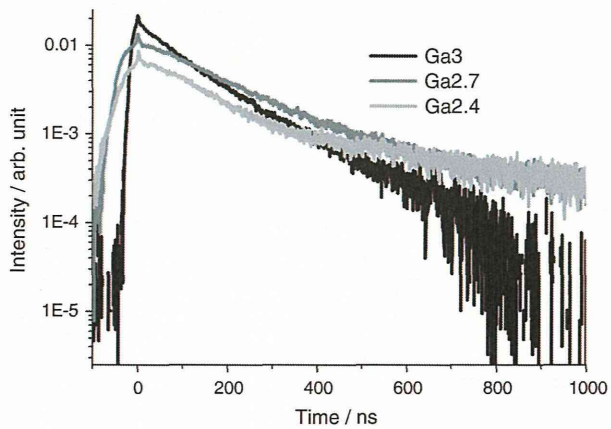

Fig. 5. Decay curves of Ce 1%:GAGG samples excited by a 662 keV gamma-ray using the PMT and digital oscilloscope.

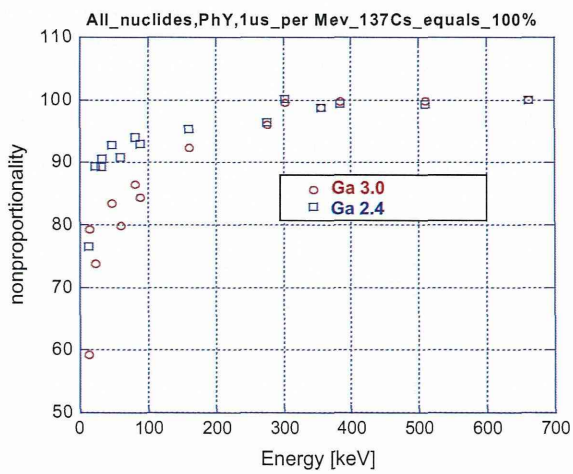

Fig. 6. Non-proportionality of the obtained samples.

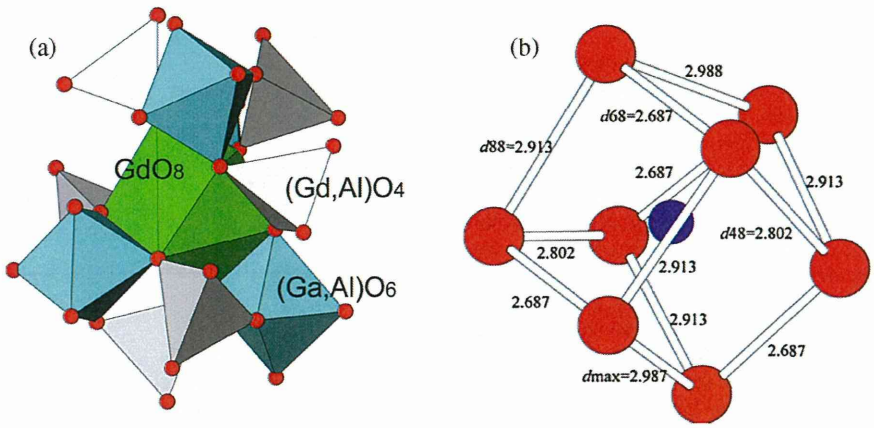

Fig. 7. (a) Schematic drawing of garnet structure of GAGG and (b) dodecahedral site.

Table 2
Interatomic distance (in Å) for $(Ce_{0.01}Gd_{0.99})_3Al_{5-x}Ga_xO_{12}$.

	Ga2.95	Ga2.65	Ga2.35	Ga2.05
Lattice constant	12.29509	12.28020	12.25216	12.24542
R factor	0.0252	0.0238	0.0233	0.0226
Dodecahedoron	2.364	2.362	2.357	2.361
	2.484	2.477	2.477	2.483
Dodecahedral_ave.	2.424	2.420	2.417	2.422
Octahedron	1.966	1.960	1.956	1.951
Tetrahedron	1.825	1.829	1.820	1.815
d68	2.687	2.675	2.676	2.677
d48	2.802	2.809	2.796	2.794
d88	2.913	2.907	2.909	2.927
d max	2.988	2.982	2.976	2.976
d ave.	2.832	2.826	2.824	2.830
Standard deviation	0.161	0.167	0.165	0.177

monochromated Mo Kα radiation ($\lambda = 0.71069$ Å) on a Rigaku AFC7R four-circle diffractometer: $h = 0 \rightarrow 22$–23, $k = 0 \rightarrow 16$, $l = 0 \rightarrow 22$–23; $2\theta_{max} = \sim 70°$; three standard reflections every 150 reflections (without intensity decay). After Lorenz and polarization corrections, absorption corrections for spherical samples were applied. The lattice constants recorded above were determined from 24 reflections with high 2θ values by the least-squares procedure. Experimental result and average distance between cation and anion in each sites in garnet structure. All R factors are well converging. Ga concentration was measured by EDX analysis in advance. As shown in Table 2, interatomic distance in tetrahedral site in Ga2.7 sample is specifically large while interatomic distance in octahedral site is gradually increase with increasing Ga concentration. Moreover, standard deviations of interatomic distances in dodecahedral site (d68, d48 and d88) showed particular value in Ga2.7. These results indicates particular occupancy of Ga^{3+} in octahedral and tetrahedral sites in Ga2.7. There are possibility that particular occupancy phenomena in Ga2.7 cause increase of its light yield. However, much more investigations and researches are necessary to explain the relationship between crystal structure and scintillation properties in Ce:GAGG.

4. Conclusion

Relationship between Ga concentration, light yield, energy resolution and crystal structure was discussed using the grown Ce 1%:$Gd_3(Al_{1-x}Ga_x)_5O_{12}$ (GAGG) single crystals with various Ga concentration of $x = 2$, 2.4, 2.7 and 3. Light yield has maximum value of 58,000 photon/MeV at $x = 2.7$ Ga concentration. Energy resolution was improved with decreasing Ga concentration and took the best value of 4.2%@662 keV at $x = 2.4$. Interatomic distance in tetrahedral site and standard deviation of anion bond length in dodecahedral site at Ga2.7 sample showed particular value compared to the other samples.

Acknowledgements

This work is partially supported by (i) the funding program for next generation world-leading researchers, JSPS, (ii) Development of Systems and Technology for Advanced Measurement and Analysis, Japan Science and Technology Agency (JST) (iii) Adaptable & Seamless Technology Transfer Program through Target-driven R&D (A-STEP), JST (iv) Japan Society for the Promotion of Science (JSPS) Grant-in-Aid for Exploratory Research (A.Y), (v) JSPS Research Fellowships for Young Scientists (S. Kurosawa) and (vi) the Health Labour Sciences Research Grant, The Ministry of Health Labour and Welfare. In addition, we would like to thank following persons for their support: Mr. Yoshihiro Nakamura in Institute of Multidisciplinary Research for Advanced Materials (IMRAM), Tohoku University and Mr. Hiroshi Uemura, Ms. Keiko Toguchi and Ms. Megumi Sasaki, Ms. Yuka Takeda in IMR.

References

[1] N.J. Cherepy, J.D. Kuntz, Z.M. Seeley, S.E. Fisher, O.B. Drury, B.W. Sturm, et al., Proc. SPIE 7805 (2010) 780501–780505.
[2] K. Kamada, T. Endo, K. Tsutumi, T. Yanagida, Y. Fujimoto, A. Fukabori, et al., Cryst. Growth Des. 11 (2011) 4484–4490.
[3] K. Kamada, T. Yanagida, J. Pejchal, M. Nikl, T. Endo, K. Tsutumi, et al., J. Phys. D: Appl. Phys. 44 (2011) 505104–505111.
[4] K. Kamada, T. Yanagida, T. Endo, K. Tsutumi, Y. Usuki, M. Nikl, et al., J. Cryst. Growth 352 (2012) 88–90.
[5] K. Kamada, T. Yanagida, J. Pejchal, M. Nikl, T. Endo, K. Tsutumi, et al., IEEE Trans. Nucl. Sci. 59 (5) (2012) 2126–2129.
[6] K. Kamada, T. Yanagida, T. Endo, K. Tsutumi, M. Yoshino, J. Kataoka, et al., J. Cryst. Growth 352 (2012) 91–94.
[7] P. Prusa, K. Kamada, M. Nikl, A. Yoshikawa, J.A. Mares, Radiation Measurements, in press, 2013, http://dx.doi.org/10.1016/j.radmeas.2013.01.055.
[8] M. Nikl, A. Vedda, M. Fasoli, I. Fontana, V.V. Laguta, E. Mihokova, et al., Phys. Rev. B 76 (2007) 195121–195128.
[9] H. Kimura, H. Maeda, M. Sato, J. Cryst. Growth 74 (January) (1986) 187–190.
[10] W.L. Bond, Rev. Sci. Instr. 22 (1951) 344.

Ann Nucl Med (2013) 27:898–906
DOI 10.1007/s12149-013-0768-7

ORIGINAL ARTICLE

Prediction of outcomes in MCI with ^{123}I-IMP-CBF SPECT: a multicenter prospective cohort study

Kengo Ito · Etsuro Mori · Hidenao Fukuyama · Kazunari Ishii · Yukihiko Washimi · Takashi Asada · Satoru Mori · Kenichi Meguro · Shin Kitamura · Haruo Hanyu · Seigo Nakano · Hiroshi Matsuda · Yasuo Kuwabara · Kazuo Hashikawa · Toshimitsu Momose · Yoshitaka Uchida · Jun Hatazawa · Satoshi Minoshima · Kenji Kosaka · Tatsuo Yamada · Yoshiharu Yonekura · J-COSMIC Study Group

Received: 7 May 2013 / Accepted: 22 August 2013 / Published online: 6 September 2013

Abstract
Objective The multicenter prospective cohort study (Japan Cooperative SPECT Study on Assessment of Mild Impairment of Cognitive Function: J-COSMIC) aimed to examine the value of ^{123}I-*N*-isopropyl-4-iodoamphetamine cerebral blood flow (IMP-CBF) SPECT in regards to early diagnosis of Alzheimer's disease (AD) in patients with mild cognitive impairment (MCI).
Methods Three hundred and nineteen patients with amnestic MCI at 41 participating institutions each underwent clinical and neuropsychological examinations and ^{123}I-IMP-CBF SPECT at baseline. Subjects were followed up periodically for 3 years, and progression to dementia was evaluated. SPECT images were classified as AD/DLB (dementia with Lewy bodies) pattern and non-AD/DLB pattern by central image interpretation and automated region of interest (ROI) analysis, respectively. Logistic regression analyses were used to assess whether baseline ^{123}I-IMP-CBF SPECT was predictive of longitudinal clinical outcome.
Results Ninety-nine of 216 amnestic MCI patients (excluding 3 cases with epilepsy ($n = 2$) or hydrocephalus ($n = 1$) and 100 cases with incomplete follow-up) converted to AD within the observation period. Central image

Electronic supplementary material The online version of this article (doi:10.1007/s12149-013-0768-7) contains supplementary material, which is available to authorized users.

K. Ito (✉) · J-COSMIC Study Group
Department of Clinical and Experimental Neuroimaging, Center for Development of Advanced Medicine for Dementia, National Center for Geriatrics and Gerontology, 35 Gengo Morioka-cho, Obu-shi, Aichi 474-8511, Japan
e-mail: kito@ncgg.go.jp

E. Mori
Department of Behavioral Neurology and Cognitive Neuroscience, Tohoku University, Sendai, Japan

H. Fukuyama
Human Brain Research Center, Kyoto University, Kyoto, Japan

K. Ishii
Department of Radiology, Kinki University, Osakasayama, Japan

Y. Washimi
Department of Outpatient Services, National Center for Geriatrics and Gerontology, Obu, Japan

T. Asada
Department of Neuropsychiatry, Institute of Clinical Medicine, University of Tsukuba, Tsukuba, Japan

S. Mori
School of Human Nursing, The University of Shiga Prefecture, Hikone, Japan

K. Meguro
Department of Geriatric Behavioral Neurology, Tohoku University, Sendai, Japan

S. Kitamura
Department of Neurology, Nippon Medical School Musashi Kosugi Hospital, Kawasaki, Japan

H. Hanyu
Department of Geriatric Medicine, Tokyo Medical University, Tokyo, Japan

S. Nakano
Sumida Hospital, Tokyo, Japan

H. Matsuda
Integrative Brain Imaging Center, National Center of Neurology and Psychiatry, Kodaira, Japan

interpretation and automated ROI analysis predicted conversion to AD with 56 and 58 % overall diagnostic accuracy (sensitivity, 76 and 81 %; specificity, 39 and 37 %), respectively. Multivariate logistic regression analysis identified SPECT as a predictor, which distinguished AD converters from non-converters. The odds ratio for a positive SPECT to predict conversion to AD with automated ROI analysis was 2.5 and combining SPECT data with gender and mini-mental state examination (MMSE) further improved classification (joint odds ratio 20.08). *Conclusions* ^{123}I-IMP-CBF SPECT with both automated ROI analysis and central image interpretation was sensitive but relatively nonspecific for prediction of clinical outcome during the 3-year follow-up in individual amnestic MCI patients. A combination of statistically significant predictors, both SPECT with automated ROI analysis and neuropsychological evaluation, may increase predictive utility.

Keywords Alzheimer's disease · Mild cognitive impairment · SPECT · Cerebral blood flow · Prospective study

Introduction

Although disease-modifying drugs such as vaccines and secretase inhibitors have been evaluated in clinical trials, essential treatment for Alzheimer's disease (AD) has not yet been established. However, with early diagnosis of AD it is possible to delay progress of symptoms through pharmacological and non-pharmacological therapy. Since pathological changes such as senile plaques begin more than a couple of decades before the manifestation of AD [1–3], diagnosis with a sophisticated method is required for early intervention.

Mild cognitive impairment (MCI) is a diagnostic entity used to describe defective memory performances that do not fulfill the criteria for dementia [4]. MCI includes incipient AD and other causes of dementia, as well as a form of cognitive impairment that does not progress to dementia and may disappear. This entity has been redefined to include amnestic MCI and non-amnestic MCI, according to the presence of an isolated objective memory deficit or of multiple or isolated extra-memory cognitive impairments [5]. This variation in MCI has been evaluated using neuropsychological tests, neuroimaging, and biologic markers. Results of clinical studies have suggested that neuropsychological tests, especially those evaluating delayed recall, might play an important role in the identification of early or preclinical AD among subjects with MCI [6–8].

SPECT studies of cerebral blood flow have reported the ability to distinguish AD converters from non-converters with high diagnostic performance in amnestic MCI patients [9–20]. Most studies showed that the presence of AD-like hypoperfusion in the posterior associative and/or posterior cingulate cortex of patients in MCI was predictive of conversion to AD within 1–3 years of the follow-up. These studies, however, were conducted among relatively small groups of subjects and follow-up times were not unified.

In the present study, data from both clinical and ^{123}I-IMP-CBF SPECT assessments within a large multicenter prospective cohort study of subjects with amnestic MCI (Japan Cooperative SPECT Study on Assessment of Mild Impairment of Cognitive Function: J-COSMIC) are reported. The objective of this study was to investigate the diagnostic value of ^{123}I-IMP-CBF SPECT findings suggesting AD-like hypoperfusion in predicting MCI conversion to AD based on a multicenter prospective study.

Methods

Ethics statement

Each subject signed an informed consent form after the nature of the procedures had been fully explained. The study was approved by the ethics committee at every participating institution (Table s-2) and was supported by the Japanese Foundation for Aging and Health.

Y. Kuwabara
Department of Radiology, Fukuoka University Hospital, Fukuoka, Japan

K. Hashikawa
Department of Cerebrovascular Disease, Osaka Minami Medical Center, Kawachinagano, Japan

T. Momose
Department of Radiology, Tokyo University, Tokyo, Japan

Y. Uchida
Department of Radiology, Chiba University, Chiba, Japan

J. Hatazawa
Department of Nuclear Medicine, Osaka University, Suita, Japan

S. Minoshima
Department of Radiology, University of Washington, Seattle, WA, USA

K. Kosaka
Yokohama Houyuu Hospital, Yokohama, Japan

T. Yamada
Department of Neurology, Fukuoka University, Fukuoka, Japan

Y. Yonekura
National Institute of Radiological Sciences, Chiba, Japan

Participants

In this multicenter prospective cohort study, subjects with amnestic MCI were recruited between January 2004 and June 2005, and followed up annually for 3 years. Subjects came from 41 specialist centers in the field of AD and dementia across Japan (Table s-2). All subjects were living independently in the community at the time of their baseline evaluation. Patients were diagnosed as having amnestic MCI according to the following criteria: (1) a subjective and/or objective memory complaint screened through the Everyday Memory Check List (EMCL) questionnaire on forgetfulness in daily activities or in recent events; (2) an objective memory impairment documented by $\leq$13 (approximately 1.5 standard deviations (SD) below normal in Japanese subjects) on the Wechsler Memory Scale–Revised Logical Memory immediate–recall (WMS-R-LM) score; (3) preservation of general cognitive functioning documented by a mini-mental state examination (MMSE) score between 24 and 30; (4) preservation of instrumental activities of daily living; (5) National Institute of Neurological and Communication Disorders and Stroke/Alzheimer's Disease and Related Disorders Association (NINCDS/ADRDA) criteria for probable AD not met; and (6) a global score on the Clinical Dementia Rating (CDR) of 0.5, memory box score of 0.5, and either 0 or 0.5 on all other box scores. Exclusion criteria were as follows: patients with history of major psychiatric or neurological disease; those with neurological signs including hemiparesis, extrapyramidal signs, bulbar palsy, ataxia, oculomotor palsy, aphasia, apraxia, agnosia, unilateral spatial neglect, and seizures; and those with psychiatric symptoms including depression, hallucinations, and delusions. Patients with small subcortical ischemic lesions that were clinically and historically silent and patients with insignificant white matter changes on MRI or CT were not excluded.

Follow-up assessment

Patients were observed at 1-year intervals for 3 years and underwent the following standardized procedures. Baseline and follow-up yearly evaluations were performed by trained clinicians. The CDR, MMSE, EMCL, and WMS-R-LM were completed at each visit during follow-up. The Alzheimer's Disease Assessment Scale cognitive subscale (ADAS) was also administered as an option in selected centers. Conversion to dementia was designated when CDR became $\geq$1. The diagnosis of AD was made in a given center when a patient fulfilled both CDR $\geq$1 and the NINCDS-ADRDA probable AD criteria. The diagnosis of other causes was based on established clinical criteria for each disease including vascular dementia (VaD) [21], dementia with Lewy bodies (DLB) [22], frontotemporal dementia (FTD) [23], and Creutzfeldt–Jakob disease (CJD) [24]. The diagnosis was further reviewed by the Clinical Diagnosis Committee composed of neurologists, psychiatrists, and a neuropsychologist (Table s-1).

SPECT

All patients underwent ^{123}I-IMP-CBF SPECT at baseline. Studies were done in a resting state with eyes closed and ears unplugged. After intravenous injection of 111 to 222 MBq dose of ^{123}I-IMP, SPECT images were acquired over a period of 15 to 45 min beginning from 10 to 30 min after administration of ^{123}I-IMP (Table s-3). Images were reconstructed using standard software as supplied by scanner manufacturers including correction for attenuation. Reconstruction conditions used during routine medical care at each facility were used.

^{123}I-IMP-CBF SPECT images were treated with the three-dimensional stereotactic surface projections (3D-SSP) technique to generate z-score maps using iSSP software version 3.5 (Nihon Medi-Physics Co. Ltd., Tokyo, Japan). In this study, a normal database of healthy subjects derived from Chiba University Hospital or National Center for Psychiatry and Neurology was used as a common database. The healthy subjects for each database had no history of neurologic or psychiatric disorders. The results of their neurologic examination and brain imaging examinations (MR imaging or CT) were normal, and their cognitive function was judged to be normal by experienced neurologists (MMSE score, 25–30). The databases chosen for further analyses of SPECT data from the corresponding institution were the databases which produced fewer artifacts on a 3D-SSP *Z* score map in a preliminary comparison between the normal database and normal subjects from each institution. The 3D-SSP program also allows group comparisons between a patient group and a normal control group, or between 2 patient groups.

Central image interpretation

To evaluate the accuracy of visual SPECT ratings to predict AD in patients with MCI, central image interpretation of SPECT data at baseline was performed by the SPECT diagnosis committee (Table s-1). Four experts, blinded to clinical information, independently assessed reconstructed SPECT images referring to a 3D-SSP *Z* score map to classify the images into AD/DLB pattern (AD pattern and DLB pattern) and non-AD/DLB pattern including FTD pattern, other neurodegenerative pattern, non-neurodegenerative pattern, and normal pattern (Fig. 1). First, raters had to make a diagnosis of either AD/DLB or non-AD/DLB and indicate their degree of diagnostic confidence on a

5-point scale, ranging from −2 (absent) to 2 (probable). Second, by focusing attention on the areas most critical to the diagnosis of AD/DLB and FTD, they had to decide which diagnosis was adopted for each case. Four specific brain regions were rated for blood flow reductions on a 2-point or 5 point scale, ranging from −2 (absent) to 2 (severe flow reduction). These areas were the precuneus and posterior cingulate gyrus, temporo-parietal cortex, frontal cortex, and visual cortex. If FTD was selected, raters had to decide whether there was significant dominancy in the degree of hypoperfusion between the frontal and temporal cortex. Finally, raters had to make a diagnosis of either progressive neurodegenerative pattern or not and indicate their degree of diagnostic confidence on a 5-point scale, ranging from −2 (absent) to 2 (probable).

Afterward, the experts discussed together to form an agreement for the cases in which classification by each expert was different. Concordance among four experts was evaluated by the method for calculation of κ index for multiple readers described by Fleiss [25].

Automated region of interest (ROI) analysis

To evaluate ROI-derived SPECT indices in predicting conversion from MCI to AD,we used a computer-assisted diagnostic system for neurodegenerative dementia using ^{123}I-IMP-CBF SPECT and 3D-SSP. The detailed procedure of this system is described elsewhere [26]. For each individual surface projection image, a Z score was calculated for each pixel and shown as a Z score map. The summed Z scores in each area of the predefined AD ROI map were calculated [26]. Threshold values were set at mean + 2 SD. For this system, a diagnosis of AD was made in any subject with at least two areas in the bilateral parietal association areas and posterior cingulate cortices where the summed Z scores exceeded the thresholds as AD. In this study, DLB was not distinguished from AD and this procedure was applied as a diagnosis of an AD converter when the subject was diagnosed with AD.

Group comparisons

To investigate specific blood flow changes occurring in each subgroup, group comparisons were performed between each subgroup classified by the central image interpretation by means of the 3D-SSP program. A group comparison between AD converters and non-converters determined by clinical outcomes during the 3-year follow-up was also performed.

Logistic regression analysis

Multivariate logistic regression analyses were used to assess whether baseline ^{123}I-IMP-CBF SPECT was predictive of longitudinal clinical outcome of development of AD. The odds of AD converters versus non-converters were estimated as a function of age, gender, education, MMSE, WMS-R-LM and SPECT. MCI patients were

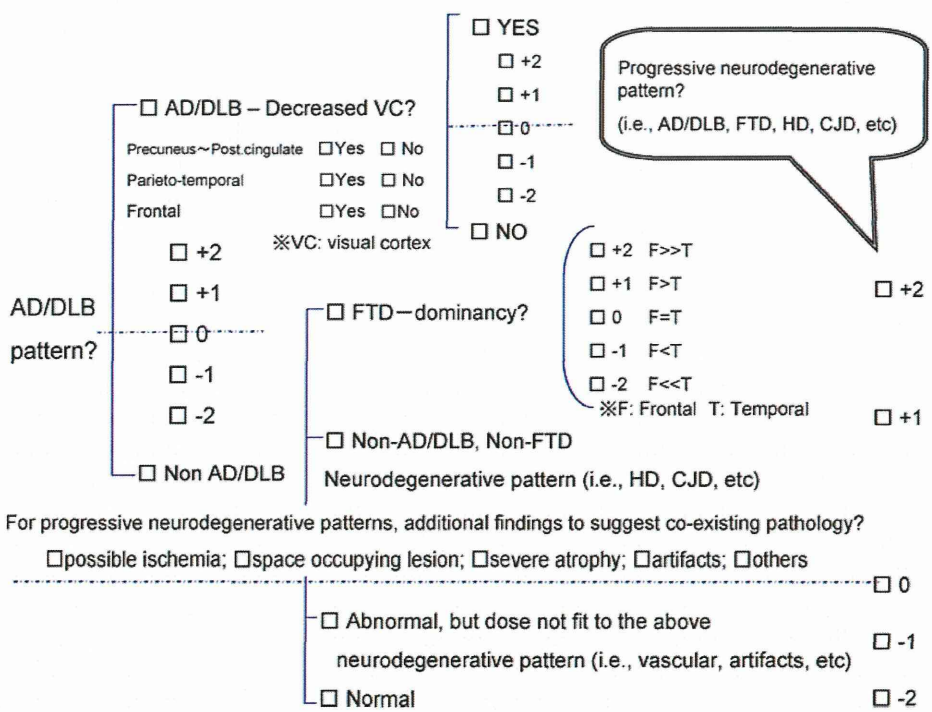

Fig. 1 Check sheet used for the central image interpretation. Each expert was asked to report the findings on SPECT images and 3D-SSP Z score maps based on this diagnostic tree. First, the images were classified into AD/DLB pattern and non-AD/DLB pattern with confidence rating, and then sub-classified in each category. Additional findings to suggest co-existing pathology were also reported

classified according to the results of image interpretation or automated ROI analysis into 2 groups: AD/DLB pattern group and non-AD/DLB pattern group. Results were considered significant at $p < 0.05$. Statistical analyses were computed with SPSS for Windows (version 14.0; SPSS Inc., Chicago, IL).

Results

Baseline characteristics and neuropsychological reevaluation

Although 319 patients fulfilled the inclusion criteria and enrolled in the study, 3 patients in whom clinical diagnosis of epilepsy ($n = 2$) or hydrocephalus ($n = 1$) was clarified thereafter were excluded from analyses. Thus, 316 patients (213 women, 103 men; mean age 73.6 ± 6.6 years) were included. Education level was 10.7 ± 2.8 years. Among these 316 patients, 100 withdrew from the study: 44 had no follow-up visits, 30 had only 1 visit, and 26 had 2 visits without conversion to dementia. Because of uncertainty about their cognitive status over time, these 100 patients who withdrew were excluded from the outcome analyses. Of the remaining 216 subjects, 103 patients converted to dementia. Alzheimer's disease was diagnosed in 99 cases and non-AD dementia in 4 cases (1 CJD, 1 FTD, and 2 VaD) (Fig. 2). As AD was the primary outcome of the study, these patients with non-AD dementia were excluded from further analyses. The annual conversion rate was 15.6 %.

There were no differences in baseline characteristics at the initial visit between those who completed follow-up and the 100 subjects who withdrew (Table 1). Demographic and neuropsychological data at the initial visit in patients who developed AD (AD converters) and those who did not (non-converters) are shown in Table 2. At baseline, the 2 groups differed in age (74.9 ± 6.4 and 72.8 ± 5.9 years in the AD converters and non-converters, respectively; $p < 0.0001$). The proportion of women was higher in AD converters than in non-converters. There was no difference between the groups in education.

SPECT

Central image interpretation and automated ROI analysis

As the result of central image interpretation, AD/DLB pattern was observed in 66.5 % (AD pattern: 47.8 %, $n = 152$; DLB pattern: 18.7 %, $n = 60$) of all amnestic

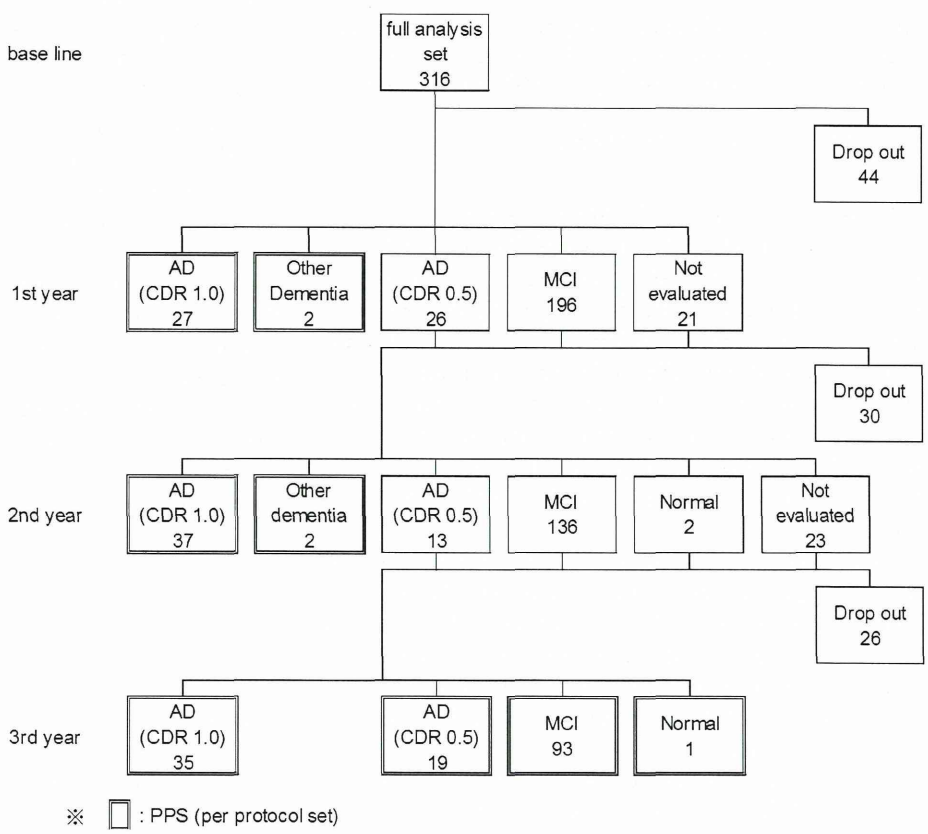

Fig. 2 Schematic summary of clinical outcomes in all MCI cases. Originally, 316 patients with MCI were included. A total of 100 patients were dropped out during 3 years. Our final sample size for the analyses of SPECT images was 214 patients excluding 4 patients who converted to other dementia

Table 1 Baseline characteristics between those whose follow-up were completed and those who were dropped out

	Completed		Dropped out	
	n	mean (SD)	*n*	Mean (SD)
Age	216	73.7 (6.3)	100	73.3 (7.3)
Sex (male:female)	216	69:147	100	34:66
Education (year)	215	10.8 (2.8)	99	10.6 (2.9)
WMS-R-LM	216	7.8 (3.5)	100	7.6 (3.5)
MMSE	216	26.4 (1.8)	100	26.3 (1.9)
ADAS	132	9.3 (4.1)	67	9.4 (4.4)
EMC	198	12.8 (6.8)	92	11.4 (5.6)

Table 2 Demographic and neuropsychological data at baseline in AD-converters and non-converters

	AD converter		Non-converter	
	n	Mean (SD)	*n*	Mean (SD)
Age*	99	74.9 (6.4)	113	72.8 (5.9)
Sex* (male:female)	99	23:76	113	43:70
Education (year)	99	10.6 (2.4)	112	11.0 (3.1)
WMS-R-LM**	99	6.2 (3.5)	113	8.7 (3.0)
MMSE***	99	25.9 (1.5)	113	26.9 (2.0)
ADAS***	63	10.7 (4.1)	71	8.0 (3.8)
EMC**	93	14.3 (7.0)	101	11.6 (6.4)

WMS-R-LM Wechsler Memory Scale–Revised Logical Memory immediate–recall, *MMSE* mini-mental state examination, *ADAS* Alzheimer's Disease Assessment Scale, *EMC* Everyday Memory Check List

* $p < 0.05$, ** $p < 0.01$, *** $p < 0.001$

MCI patients. Non-AD/DLB pattern, on the other hand, was observed in 33.5 % (including FTD pattern in 8.5 %, $n = 27$) (Fig. 3). Inter-rater agreement was moderate ($\kappa = 0.43$) for SPECT image interpretation based on 5 patterns (AD, DLB, FTD, other neurodegenerative pattern and non-neurodegenerative and normal pattern). For the purpose of statistical analysis, non-neurodegenerative pattern and normal pattern were grouped together. There was no significant difference in pattern classification between those who completed follow-up and the 100 subjects who withdrew.

Image interpretation based on the classification of SPECT images predicted conversion to AD with an overall diagnostic accuracy of 56 %, sensitivity of 76 %, and specificity of 39 % for the data set of 212 subjects in this study. For calculation of diagnostic performance, the AD pattern and the DLB pattern were combined as the AD/DLB pattern (Table 3).

Diagnostic performance of the automated ROI analysis was applied in this study with an overall diagnostic accuracy of 58 %, a sensitivity of 81 %, and specificity of 37 % for differentiation of AD converters from non-converters (Table 3).

Group comparisons

The 3D-SSP displays in Fig. 3 show the results of group comparisons between the progressive neurodegenerative pattern groups (AD pattern group, DLB pattern group and FTD pattern group) and the normal pattern group classified by central image interpretation. Each progressive neurodegenerative pattern group demonstrated a decrease in cerebral blood flow in the regions typical for AD, DLB and FTD.

Group comparison between AD converters and non-converters revealed that hypoperfusion was accentuated in AD converters compared to non-converters bilaterally in the temporo-parietal area, medial temporal area, and posterior cingulate and precuneus (Fig. 4).

Logistic regression analysis

Multivariate logistic regression analysis identified SPECT with automated ROI analysis as a predictor that distinguished AD converters from non-converters. When age, gender, education, MMSE and SPECT were submitted to the stepwise selection procedure, being an AD converter was significantly associated with gender (female, $p = 0.009$; odds ratio (OR) 2.36; 95 % confidence interval (CI) 1.24–4.53), MMSE (≤ 27, $p < 0.001$; OR 3.39; 95 % CI 1.71–6.75) and SPECT with automated ROI analysis (AD/DLB, $p = 0.008$; OR 2.51; 95 % CI 1.28–4.96), but not with age, education, and SPECT with central image interpretation (Table 4). The combination of gender, MMSE, and SPECT with automated ROI analysis further improved classification (joint OR 20.08). When WMS-R-LM was submitted instead of MMSE, being an AD converter was significantly associated with gender (female, $p = 0.006$; OR 2.56; 95 % CI 1.32–5.00), WMS-R-LM (≤ 7, $p < 0.001$; odds ratio 4.10; 95 % CI 2.26–7.47) and SPECT with automated ROI analysis (AD/DLB, $p = 0.004$; OR 2.72; 95 % CI 1.36–5.41) (Table 4). Consequently, the joint OR was 28.44.

Discussion

In the present study, 99 (46.7 %) of 212 MCI patients converted to AD and the annual conversion rate was 15.6 % during the 3-year follow-up. The present results are consistent with reports from other groups indicating that 12–15 % of amnestic MCI patients annually convert to AD [4].

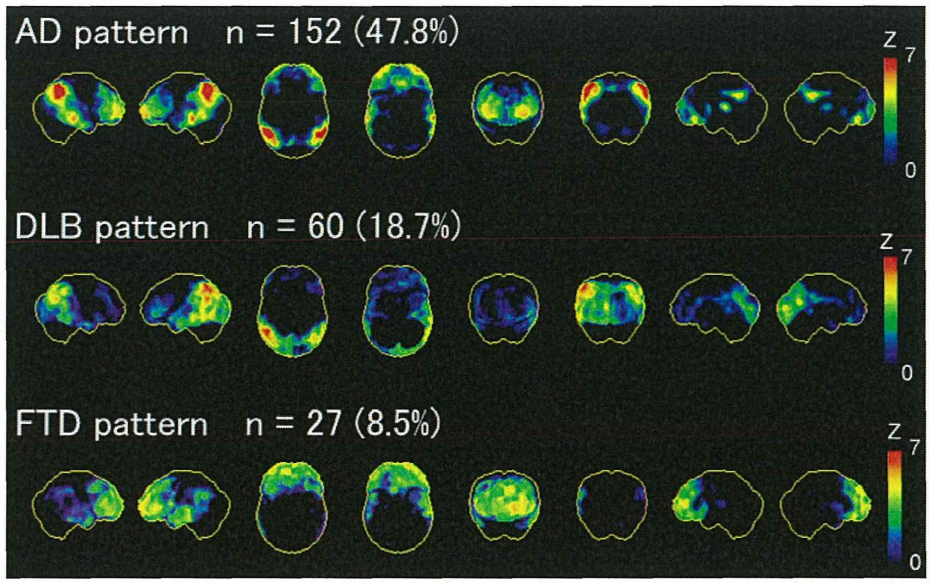

Fig. 3 3D-SSP *Z* score maps showing hypoperfusion in the progressive neurodegenerative pattern groups (AD, DLB and FTD pattern groups) compared to the normal pattern group. Numbers of each pattern indicate number of cases classified by central image interpretation. From *left to right*: 3D-SSP maps are shown on the right and left lateral views, superior and inferior views, anterior and posterior views, and right and left middle views of a standardized brain image

Table 3 Discrimination between AD converter and non-converter in MCI by baseline ^{123}I-IMP-CBF SPECT

Type of analysis	Sensitivity	Specificity	PPV	NPV	Accuracy
Central image interpretation	76 % (75/99)	39 % (44/113)	52 % (75/144)	64 % (4 4/68)	56 % (119/212)
Automated ROI analysis	81 % (80/99)	37 % (42/113)	53 % (80/151)	69 % (42/61)	58 % (122/212)

PPV positive predictive value, *NPV* negative predictive value

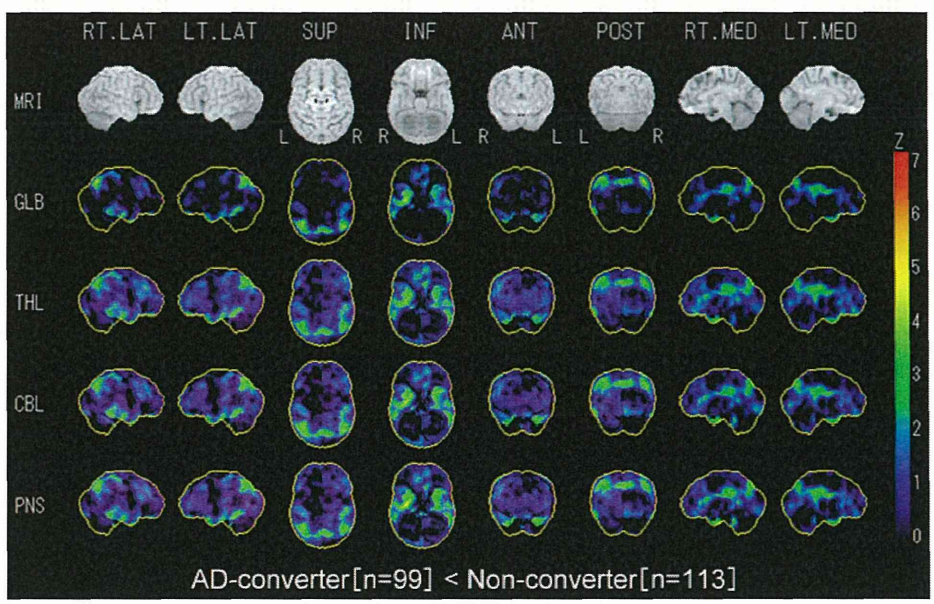

Fig. 4 3D-SSP *Z* score maps showing hypoperfusion in AD converters compared to non-converters. Hypoperfusion is observed in the regions affected typically in AD, but not prominent. It may be caused by the existence of cases showing AD pattern in non-converters. From *left to right*: 3D-SSP maps are shown on the right and left lateral views, superior and inferior views, anterior and posterior views, and right and left middle views of a standardized brain image

The present study demonstrated that ^{123}I-IMP-CBF SPECT with automated ROI analysis was a predictor for conversion to AD among amnestic MCI patients across institutions where various types of gamma cameras were used. Furthermore, improved predictive power resulted after inclusion of gender and a neuropsychological

Table 4 Result of Multivariate logistic regression analyses for predictors of AD converter

Variable	Coefficient (*B*)	SE	Wald	*df*	*p* value	Odds ratios	95 % CI
Gender (female)	0.86	0.33	6.75	1	0.009	2.36	1.24–4.53
MMSE ≦27	1.22	0.35	12.12	1	<0.001	3.39	1.71–6.75
SPECT with automated ROI analysis	0.92	0.35	7.08	1	0.008	2.51	1.27–4.96
Constant	−2.28	0.48	22.79	1	<0.001	0.1	
Variable	Coefficient (*B*)	SE	Wald	*df*	*p* value	Odds ratios	95 % CI
Gender (female)	0.94	0.34	7.66	1	0.006	2.56	1.32–5
WMS-R-LM ≦7	1.41	0.31	21.36	1	<0.001	4.10	2.26–7.47
SPECT with automated ROI analysis	1.00	0.35	8.07	1	0.004	2.72	1.36–5.41
Constant	−2.18	0.45	23.57	1	<0.001	0.11	

df degree of freedom, *CI* confidence interval, *MMSE* mini-mental state examination, *WMS-R-LM* Wechsler Memory Scale–Revised Logical Memory immediate–recall

evaluation (such as MMSE and WMS-R-LM). Although WMS-R-LM was more powerful predictor than MMSE, MMSE is a neuropsychological evaluation generally performed for screening the cognitive functions at memory clinics. Therefore, the combination of both MMSE and SPECT is more practical as a routine clinical scenario. An early high- or low-risk stratification of amnestic MCI patients could assist in the early intervention of AD.

Central image interpretation of ^{123}I-IMP-CBF SPECT failed to identify SPECT as a predictor for development of AD in logistic regression analysis. This failure could be caused by the difficulty of reviewing SPECT and 3D-SSP *Z* score maps with heterogeneous image qualities from various types of gamma cameras from 41 institutions. Furthermore, there were some artifacts on 3D-SSP *Z* score maps due to the use of a common normal database in this study. The artifacts made it difficult to identify true hypoperfusion areas. SPECT images should be standardized and more sophisticated normal databases should be used for further study. However, quantitative evaluation, such as automated ROI analysis, might be more robust and accurate than visual inspection for a dataset of SPECT images from multiple centers.

^{123}I-IMP-CBF SPECT with both automated ROI analysis and central image interpretation was sensitive but relatively nonspecific for prediction of clinical outcome during the 3-year follow-up in individual amnestic MCI patients. Problems in prediction included low specificity (central image interpretation, 39 %; automated ROI analysis, 37 %), which resulted in a significant number of false-positive cases on SPECT images in non-converters. These results were not in line with previous reports [9–20] where higher specificity and diagnostic accuracy were reported. The true reason having low specificity in spite of a longer follow-up compared to previous reports is unclear. One possible reason is difference in the characteristics of registered MCI patients for each study. In fact conversion rates from MCI to AD were very high in some studies. Increase of the ratio of converters may result to a decrease of false-positive cases. In addition, heterogeneous image quality due to scanner differences in a multicenter study and artifacts on 3D-SSP *Z* score maps due to use of a common normal database might affect the specificity of both central image interpretation and automated ROI analysis. In this study ^{123}I-IMP was adopted for SPECT study. Cerebral blood flow SPECT with ^{123}I-IMP is widely used in Japan. Though it cannot be denied that there are some differences in image quality between ^{123}I-IMP and ^{99m}Tc labeled tracers, there is no study reporting that the diagnostic accuracy of ^{123}I-IMP is inferior to that of ^{99m}Tc labeled tracers.

Although the annual conversion rate to AD was 15.6 % during the present 3-year study, conversion after 3 years is also possible and expected. With longer follow-up, amnestic MCI patients might develop cognitive deficits and eventually convert to AD. Therefore, improvement of specificity and diagnostic accuracy can be expected due to a decrease of false-positive cases provided by a longer follow-up period.

Group comparison based on classification of the central image interpretation demonstrated heterogeneity in ^{123}I-IMP-CBF SPECT of cerebral blood flow among subjects with amnestic MCI. Although the progressive pattern included the AD pattern (47.8 %), the DLB pattern (18.7 %) and the FTD pattern (8.5 %), 99 (96.1 %) of 103 converters were AD converters without any case converted to DLB. Therefore, we believe that combining AD pattern with DLB pattern as AD/DLB pattern to investigate the role of ^{123}I-IMP-CBF SPECT in predicting conversion to AD is not problematic. The clinical significance of the heterogeneity in ^{123}I-IMP-CBF SPECT should be further evaluated. In a group comparison between AD converters